Hindawi
Advances in Materials Science and Engineering
Volume 2019, Article ID 6204145, 10 pages
https://doi.org/10.1155/2019/6204145

Research Article

Geometrically Nonlinear Analysis of Functionally Graded Timoshenko Curved Beams with Variable Curvatures

Ze-Qing Wan, Shi-Rong Li, and Hong-Wei Ma

College of Civil Science and Engineering, Yangzhou University, Yangzhou, China

Correspondence should be addressed to Ze-Qing Wan; zqwan@yzu.edu.cn

Received 22 January 2019; Accepted 7 May 2019; Published 9 June 2019

Guest Editor: Saifulnizan B. Jamian

In this paper, geometrically nonlinear analysis of functionally graded curved beams with variable curvatures based on Timoshenko beam theory is presented. Considering the axial extension and the transversal shear deformation, geometrically nonlinear governing equations for the FGM curved beams with variable curvatures subjected to thermal and mechanical loads are formulated. Material properties of the curved beams are assumed to vary arbitrarily in the thickness direction and be independent on the temperature change. By using the numerical shooting method to solve the coupled ordinary differential equations, the nonlinear response of static thermal bending of a FGM semielliptic beams subjected to transversely nonuniform temperature rise is obtained numerically. The effects of material gradient, shear deformation, and temperature rise on the response of the curved beam are discussed in detail. Nonlinear bending of a closed FGM elliptic structure subjected to two pinching concentrated loads is also analyzed. This paper presents some equilibrium paths and configurations of the elliptic curved beam for different pinching concentrated loads.

1. Introduction

Curved beams have been widely applied in many engineering disciplines such as civil, mechanical, and aerospace [1]. For instance, robotic arms, coil laminated springs, and reinforced stiffeners in aircraft structures are generally designed as curved beams. For another example, golf shafts and fishing rods have apparently deformed shapes during use, both of which can be analyzed by curved beam theory. The analysis of static, stability, and dynamic behavior of curved beam structures was frequently performed by researchers. However, as the extending of application range of curved beams, the performance of traditional composite materials cannot meet the increasing requirements. To adapt to high temperature environment, functionally graded material (FGM) may be suggested. FGM structures become increasingly attractive in many engineering applications [2]. Typically, these materials consist of a mixture of ceramic and metal or a combination of different materials. The mechanical properties vary smoothly and continuously from one surface to another. It has many good performances in engineering applications, such as high resistance to large temperature gradients and reduction of stress concentration [3].

There have been lots of literatures on geometrically nonlinear analysis of curved beams. Pi and Bradford [4, 5] presented a theoretical analysis of the nonlinear elastic in-plane behavior and buckling of a pinned-fixed curved beam subjected to a radial load distributed uniformly around the beam axis and a central concentrated radial load, respectively. Liu and Lu [6] formulated a variational framework for large-displacement space curved beams by considering geometric nonlinearity and different scalings of kinematic variables. Based on a new variational principle expressed in terms of stress components, Cannarozzi and Molari [7] proposed a nonlinear formulation for curved, extensible, shear flexible, elastic planar beams. The research of curved beams considering the extension of axis length was also conducted by Pulngern et al. [8]. In their work, the postbuckling behaviors of a variable-arc-length circular curved beam subjected to an end follower force were examined by using the elliptic integrals method and shooting method.

In the above-cited references, one can note that the material properties of curved beams were assumed to be homogeneous. Extensive nonlinear analysis of the mechanics of straight FGM beams has been done in order to understand the nonlinear static and dynamic responses of FGM beams [9–11]. However, the published papers which have been devoted to FGM curved beams are fewer. Based on the classical beam theory along with the nonlinear shallow shell theory of Donnell, Asgari et al. [12] presented a theoretical investigation on the thermoelastic behavior of pin-ended FGM circular shallow arches. Temperature dependency of constituents was taken into account, and the arch was subjected to a uniform temperature field. In the study of Bateni and Eslami [13, 14], they studied the nonlinear stability behavior of FGM circular shallow arches subjected to a central concentrated force and a uniform radial pressure, respectively. Numerical results were presented as the influences of material dispersion, geometrical characteristics, and boundary conditions on the stability behavior of the FGM circular shallow arches. Based on the first-order shear deformation theory and von Karman geometrically nonlinear theory, Kerdegarbakhsh et al. [15] studied the buckling and postbuckling behaviors of a ring made of a through-the-thickness FGM. Kurtaran [16] performed a large displacement static and transient analysis of thick FGM curved beams by using generalized differential quadrature method. Large displacements were taken into account through Green-Lagrange nonlinear strain-displacement relations. Equilibrium equations were obtained by using virtual work principle and solved with Newton and Newmark methods for static and dynamic problems, respectively. Eroglu [17] examined the large in-plane deflections of planar curved beams made of FGM using variational iteration method. In the study, axial and shear deformations were taken into account.

Note that the abovementioned research works are limited on curved beams with constant curvature; thus, the problems can be simplified by ignoring the variable curvature effect in integrations. However, it is generally known that the curved beams with variable curvatures have been widely applied in engineering structures. Consequently, considerable research efforts have been made for the improved analysis of curved beams. Moghaddasie and Stanciulescu [18] investigated the equilibrium paths and locus of critical points based on a modified Bernoulli beam theory with large transversal displacements for a half-sine pinned curved beam under transversal loading in a thermal environment. In the study of Kim et al. [19], an improved formulation for free vibration and spatial stability of nonsymmetric thin-walled curved beams was presented based on the displacement field considering variable curvature effects and the second-order terms of finite-semitangential rotations. Lin and Lin [20] used Lagrangian description together with Eulerian description to derive analytical solutions of laminated curved beams with variable curvature under pure bending and axial forces. Luu and Lee [21] considered geometrically nonlinearity in their buckling and postbuckling analyses of elliptic curved beams subjected to a central concentrate vertical load under clamped-clamped, hinged-hinged, and clamped-hinged boundary conditions. Recently, Huynh et al. [22] investigated the bending, buckling, and free vibration of FGM curved beams with variable curvatures using isogeometric approach, based on Timoshenko curved beam theory. Four shapes of curved beams with variable curvature including circular, cycloid, elliptic, and parabolic were considered. The nonuniform rational B-spline basis functions were used in representing the geometry and approximating the unknown fields. Based on the static bending and free vibration analysis of FG microbeams by using isogeometric approach in combination with the quasi-3D beam theory, the research work about analyzing mechanical behavior of FG curved beams employing the same method is attracting great attention [23, 24].

As is well known, nonlinear mechanical performance of curved beam is very complex because the normal displacement, tangential displacement, and rotation are coupled in the differential governing equations. From the previously cited references, one can note that despite extensive research for the static and dynamical behaviors of the curved beams, to the knowledge of authors, not much work has been devoted to the geometrically nonlinear analysis of functionally graded curved beams with variable curvature. In this paper, by considering axial extension and transversely shearing, the nonlinear governing equations of FGM Timoshenko curved beams with variable curvatures subjected to thermo-mechanical loads will be presented. Then, the shooting method is applied to numerically solve the nonlinear boundary value problem. In order to illustrate the validity and practicability of the present method, numerical examples for FGM elliptic curved beams under thermal and mechanical loadings are analyzed. The effects of material gradient, shear deformation, and temperature rise on the response of the curved beams are investigated. Some equilibrium paths and configurations of FGM elliptic curved beams under different pinching concentrated loads are presented.

2. Theoretical Formations

2.1. Material Properties of FGM. We consider a FGM curved beam with rectangular cross sections, made of two isotropic constituents with the material properties P_{i} and P_{o}. The effective material properties (including Young's modulus E, Poisson's ratio ν, thermal expansion coefficient α, and the thermal conductivity coefficient K) of the FGM curved beam are assumed to be varied continuously in the thickness direction from the inner surface with P_{i} to the outer surface with P_{o}. Furthermore, the material property gradient profiles in the thickness direction are specified by the power law functions, and then the effective material properties of the FGM can be expressed in the unified power law form as

$$P(\rho) = P_{\mathrm{i}}\psi_{\mathrm{P}}(\rho), \quad \frac{-h}{2} \le \rho \le \frac{h}{2}, \tag{1}$$

where

$$\psi_{\mathrm{P}}(\rho) = 1 + (f_{\mathrm{P}} - 1)\left(\frac{1}{2} + \frac{\rho}{h}\right)^{n}, \tag{2}$$

where h denotes the thickness; $f_P = P_o/P_i$; P_i and P_o denote the material properties at the inner ($\rho = -h/2$) and the outer ($\rho = h/2$) surfaces, respectively; and n is the volume fraction exponent ($0 \le n < \infty$), especially, $n = 0$ and $n \longrightarrow \infty$ representing the two kinds homogeneous material curved beam made of the pure outer and the inner surface materials, respectively.

2.2. Geometrical Equations. Consider an arbitrary plane curved beam element with variable curvature with uniform cross section as shown in Figure 1. Choose Cartesian coordinate systems (x, z) and (X, Z) to position the points at the initial and the deformed configurations of the central axis of the curved beam, respectively. Herein, it is assumed that the geometrical central axis still remains in $x-z$ plane in the deformed state. When the beam is deformed, the material point C moves to the point $C' : (X, Z) = (x + u, z + w)$, where $u(x)$ and $w(x)$ are displacements of the point C in $x-$ and $z-$directions, respectively. At the same time, we choose the arc length coordinate, s_0 and s_0^*, to measure the central axis of the curved beam in the undeformed and deformed states, respectively. So, the relationship between the differential beam elements in the deformed and undeformed states is given by

$$ds_0^* = \sqrt{(dX)^2 + (dZ)^2} = \Lambda_0 ds_0, \tag{3}$$

where Λ_0 is the stretching of the axis expressed by

$$\Lambda_0 = \sqrt{\left(\frac{dx}{ds_0} + \frac{du}{ds_0}\right)^2 + \left(\frac{dz}{ds_0} + \frac{dw}{ds_0}\right)^2}. \tag{4}$$

If we ignore the axial extension of the beam, then we have $\Lambda_0 \equiv 1$, or $ds_0^* = ds_0$.

By accurately considering the axial extension, the kinematics relations of the deformed central axis of the curved beam are derived as follows [25]:

$$\begin{aligned} \frac{ds_0^*}{ds_0} &= \Lambda_0, \\ \frac{du}{ds_0} &= \Lambda_0 \cos\theta - \cos\theta_0, \\ \frac{dw}{ds_0} &= \Lambda_0 \sin\theta - \sin\theta_0, \end{aligned} \tag{5}$$

where θ_0 and θ are the angles of the differential line elements, ds_0 and ds_0^*, with the x-axis, respectively.

Based on Timoshenko beam theory, the cross sections are assumed to remain plane in the course of deformation. Then, we attain the normal and the shearing strains at arbitrary point in the cross section, respectively:

$$\begin{aligned} \varepsilon &= \frac{\varepsilon_0 + \rho\kappa_1^*}{1 + \rho\kappa_0}, \\ \gamma &= \Lambda_0 \sin\gamma_0, \end{aligned} \tag{6}$$

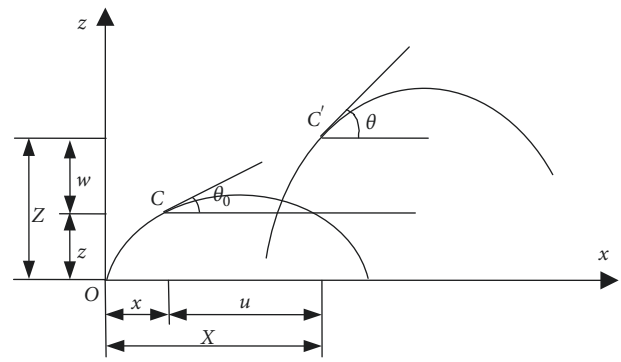

Figure 1: Schematic diagram of the curved beam's geometry.

where ε_0 is the normal strain of the central axis and κ_0 and κ_1^* denote the initial curvature and the curvature increment of the central axis of the curved beam, respectively. For the curved beam with variable curvature, both κ_0 and κ_1^* are functions of the arc length s_0. They are given by

$$\begin{aligned} \varepsilon_0 &= \Lambda_0 \cos\gamma_0 - 1, \\ \kappa_0 &= \frac{d\theta_0}{ds_0}, \\ \kappa_1^* &= \frac{d\psi}{ds_0}, \end{aligned} \tag{7}$$

where γ_0 is the shear angle and ψ is the rotational angle of the cross section. Denoting φ as the angle between the normal of the curved beam's cross section and the x-axis in the deformed state, we obtain the following relations:

$$\begin{aligned} \varphi &= \theta + \gamma_0, \\ \psi &= \varphi - \theta_0. \end{aligned} \tag{8}$$

2.3. Constitutive Equations. For the linear thermoelastic material, the stress-strain relations are given by Hook's law as follows:

$$\begin{aligned} \sigma &= E(\varepsilon - \alpha T), \\ \tau &= \frac{E}{2(1+\nu)}\gamma, \end{aligned} \tag{9}$$

where T is the temperature rise. We assume that the temperature rise changes nonhomogeneously along the thickness of the curved beam; then, it is governed by one-dimensional steady-state heat conduction equation of

$$\frac{d}{d\rho}\left[K(\rho)\frac{dT(\rho)}{d\rho}\right] = 0. \tag{10}$$

By integrating equation (10) and using the associated boundary conditions $T(h/2) = T_o$ and $T(-h/2) = T_i$, the temperature rise field in the curved beam can be expressed as follows:

$$T(\rho) = T_i \psi_T(\rho), \tag{11}$$

with

$$\psi_{\mathrm{T}}(\rho) = 1 + (f_{\mathrm{T}} - 1)\frac{\int_{-h/2}^{\rho}(1/K(\rho))d\rho}{\int_{-h/2}^{h/2}(1/K(\rho))d\rho}, \tag{12}$$

where $f_{\mathrm{T}} = T_{\mathrm{o}}/T_{\mathrm{i}}$ is the ratio of the temperature rise at the outer to that at the inner surfaces of the curved beam with $f_{\mathrm{T}} = 1$ representing the uniform temperature rise.

Substituting equation (6) into (9) and taking integration over the cross section, we obtain the axial and shear resultant forces N and Q and bending moment M as follows:

$$N = \iint_A \sigma\, dA = A_1\varepsilon_0 + B_1\kappa_1^* - N_{\mathrm{T}}, \tag{13}$$

$$M = \iint_A \sigma z\, dA = B_1\varepsilon_0 + D_1\kappa_1^* - M_{\mathrm{T}}, \tag{14}$$

$$Q = \frac{1}{k}\iint_A \tau\, dA = \frac{1}{k}S_1\Lambda_0\sin\gamma_0, \tag{15}$$

where k is the Timoshenko shear correction factor, which depends on the shape of the cross section of the beam and A_1, B_1, D_1 and S_1 are stiffness coefficients to be defined as

$$(A_1, B_1, D_1) = \iint_A \left(\frac{1}{1+\rho\kappa_0}, \frac{\rho}{1+\rho\kappa_0}, \frac{\rho^2}{1+\rho\kappa_0}\right)E(\rho)dA, \tag{16}$$

$$S_1 = \iint_A \frac{E(\rho)}{2(1+\nu)}dA, \tag{17}$$

where N_{T} and M_{T} are the thermal axial force and the thermal bending moment, given by

$$(N_{\mathrm{T}}, M_{\mathrm{T}}) = \iint_A (1, \rho)E(\rho)\alpha(\rho)T(\rho)dA. \tag{18}$$

Substitution of Young's modulus and thermal expansion coefficient in the form of equations (1) and (11) into equations (16)–(18) yields

$$(A_1, B_1, D_1, S_1) = \left(A\phi_1, Ah\phi_2, I\phi_3, \frac{A\phi_4}{2(1+\nu)}\right)E_{\mathrm{i}}, \tag{19}$$

$$(N_{\mathrm{T}}, M_{\mathrm{T}}) = (\beta_1, h\beta_2)AE_{\mathrm{i}}\alpha_{\mathrm{i}}T_{\mathrm{i}}, \tag{20}$$

where E_{i} and α_{i} are, respectively, Young's modulus and thermal expansion coefficient at the inner surface of the curved beam and A and I are the area and inertia moment of the cross section, respectively. Dimensionless coefficients ϕ_j $(j = 1, 2, 3, 4)$ and β_j $(j = 1, 2)$ are defined in Appendix.

From equations (13)–(15), we arrive at the other kinds of constitutive equations:

$$\kappa_1^* = \frac{[-B_1(N + N_{\mathrm{T}}) + A_1(M + M_{\mathrm{T}})]}{C}, \tag{21a}$$

$$\varepsilon_0 = \frac{[D_1(N + N_{\mathrm{T}}) - B_1(M + M_{\mathrm{T}})]}{C}, \tag{21b}$$

$$\Lambda_0\sin\gamma_0 = \frac{kQ}{S_1}, \tag{21c}$$

where $C = A_1D_1 - B_1^2$.

2.4. Equilibrium Equations. In the deformed state, the curved beam is assumed to be in static equilibrium. The equilibrium equations governing geometrically nonlinear deformation of Timoshenko curved beam can be derived by considering the deformed segment ds_0^* as follows:

$$\begin{aligned} dH &= q_x ds_0^*, \\ dV &= q_z ds_0^*, \\ dM &= (V\cos\theta - H\sin\theta)ds_0^*. \end{aligned} \tag{22}$$

By virtue of the first formula of equation (5), one can get Lagrange forms of equation (22) as follows:

$$\begin{aligned} \frac{dH}{ds_0} &= \Lambda_0 q_x, \\ \frac{dV}{ds_0} &= \Lambda_0 q_z, \\ \frac{dM}{ds_0} &= \Lambda_0(V\cos\theta - H\sin\theta), \end{aligned} \tag{23}$$

where H and V are the horizontal and vertical resultant forces, respectively, and q_x and q_z are components of the distributed force along the beam in the $x-$ and the $z-$axis, respectively. The resultant forces (H, V), being equivalent to (N, Q), can be expressed as

$$\begin{aligned} N &= -H\cos\varphi - V\sin\varphi, \\ Q &= H\sin\varphi - V\cos\varphi. \end{aligned} \tag{24}$$

Substituting equation (24) into equations (21a)–(21c) yields

$$\begin{aligned} \frac{d\psi}{ds_0} = \frac{1}{C}[&-B_1(-H\cos\varphi - V\sin\varphi + N_T) \\ &+ A_1(M + M_{\mathrm{T}})], \end{aligned} \tag{25}$$

$$\begin{aligned} \Lambda_0\cos\gamma_0 = \frac{1}{C}[&D_1(-H\cos\varphi - V\sin\varphi + N_{\mathrm{T}}) \\ &- B_1(M + M_{\mathrm{T}})] + 1, \end{aligned} \tag{26}$$

$$\Lambda_0\sin\gamma_0 = \frac{k}{S_1}(H\sin\varphi - V\cos\varphi). \tag{27}$$

So far, we finally arrive at the governing equations of the geometrically nonlinear deformations of FGM Timoshenko curved beams with variable curvatures subjected to thermal and mechanical loads, consisting of equations (5), (23), and (25) in terms of the seven basic unknown functions s_0^*, u, w, H, V, M, and ψ. The axial stretching Λ_0 and shearing angle γ_0 can be also expressed in terms of the above-mentioned seven unknown functions.

3. Dimensionless Governing Equations

The following dimensionless quantities are introduced:

$$(S_0, S, U, W, \lambda) = \frac{1}{L}(s_0, s_0^*, u, w, h), \tag{28a}$$

$$\begin{aligned}(Q_x, Q_z) &= \frac{L^3}{E_i I}(q_x, q_z),\\ (P_H, P_V, n_T) &= \frac{L^2}{E_i I}(H, V, N_T),\\ (m, m_T) &= \frac{L}{E_i I}(M, M_T),\end{aligned} \tag{28b}$$

$$\begin{aligned}(\eta_1, \eta_2, \eta_3) &= \frac{E_i I}{C}\left(A_1, \frac{B_1}{L}, \frac{D_1}{L^2}\right),\\ \eta_4 &= \frac{E_i I}{S_1 L^2},\end{aligned} \tag{28c}$$

where L is a characteristic length of the curved beam, which can be the main radius or the length of the central axis of the curved beam.

Thus, the dimensionless thermal axial force and thermal bending moment can be expressed as

$$\begin{aligned}n_T &= \tau_i \beta_1,\\ m_T &= \tau_i \lambda \beta_2,\end{aligned} \tag{29}$$

where τ_i is used as the reference thermal load parameter, which represents the dimensionless temperature rise of the homogeneous curved beam made of the pure inner surface material. It is defined as

$$\tau_i = \frac{12\alpha_i T_i}{\lambda^2}. \tag{30}$$

Substituting equations (28a)–(28c) into equations (5), (23), and (25), the governing equations can be transformed into the dimensionless forms as follows:

$$\begin{aligned}\frac{dS}{dS_0} &= \Lambda_0,\\ \frac{dU}{dS_0} &= \Lambda_0 \cos\theta - \cos\theta_0,\\ \frac{dW}{dS_0} &= \Lambda_0 \sin\theta - \sin\theta_0,\end{aligned} \tag{31}$$

$$\begin{aligned}\frac{dP_H}{dS_0} &= \Lambda_0 Q_x,\\ \frac{dP_V}{dS_0} &= \Lambda_0 Q_z,\\ \frac{dm}{dS_0} &= \Lambda_0 (P_V \cos\theta - P_H \sin\theta),\end{aligned} \tag{32}$$

$$\frac{d\psi}{dS_0} = -\eta_2(-P_H \cos\varphi - P_V \sin\varphi + n_T) + \eta_1(m + m_T), \tag{33}$$

where

$$\begin{aligned}\cos\theta &= \cos\varphi\ \cos\gamma_0 + \sin\varphi\ \sin\gamma_0,\\ \sin\theta &= \sin\varphi\ \cos\gamma_0 - \cos\varphi\ \sin\gamma_0,\end{aligned} \tag{34a}$$

$$\begin{aligned}\cos\varphi &= \cos\theta_0 \cos\psi - \sin\theta_0 \sin\psi,\\ \sin\varphi &= \sin\theta_0 \cos\psi + \cos\theta_0 \sin\psi,\end{aligned} \tag{34b}$$

$$\begin{aligned}\Lambda_0 &= \sqrt{\Delta_1^2 + \Delta_2^2},\\ \tan\gamma_0 &= \frac{\Delta_2}{\Delta_1},\end{aligned} \tag{34c}$$

$$\begin{aligned}\Delta_1 = {} & \eta_3(-P_H \cos\varphi - P_V \sin\varphi + n_T)\\ & - \eta_2(m + m_T) + 1,\end{aligned} \tag{34d}$$

$$\Delta_2 = k\eta_4(P_H \sin\varphi - P_V \cos\varphi), \tag{34e}$$

$$\begin{aligned}\eta_1 &= \frac{1}{\phi_3 - (12\phi_2^2/\phi_1)},\\ \eta_2 &= \frac{\lambda}{(\phi_1\phi_3/\phi_2) - 12\phi_2},\\ \eta_3 &= \frac{\lambda^2}{12(\phi_1 - (12\phi_2^2/\phi_3))},\\ \eta_4 &= \frac{(1+\nu)\lambda^2}{6\phi_4}.\end{aligned} \tag{34f}$$

From equation (34c), it can be seen that the shear deformation is relevant to parameter Δ_2. If $\Delta_2 = 0$, or η_4 tends to zero, then we have $\gamma_0 = 0$ and $\varphi = \theta$. In this case, the governing equations (31)–(33) reduce to those of FGM Euler–Bernoulli curved beams.

4. Numerical Examples

In this section, numerical results for thermal and mechanical bending of FGM elliptic curved beam composed of ceramic (ZrO_2) and metal (Al) are presented. The outer surface of the curved beam is fully ceramic and the inner surface is fully metal. The material properties of the two constituents are listed in Table 1. The effective material properties of the FGM curved beam are given by equations (1) and (2).

As the first example, we consider a FGM semielliptic curved beam made with the two ends completely clamped, which is shown in Figure 2. The beam is only subjected to thermal load given by equations (11) and (29).

The parametric equations of the semielliptic beam are given as follows:

$$\begin{aligned}x &= a\cos\zeta,\\ z &= b\sin\zeta,\\ 0 &\le \zeta \le \pi.\end{aligned} \tag{35}$$

Then, the dimensionless arc length element of the curved beam can be given by

Table 1: Material properties of the FG curved beams.

Property	E (GPa)	$\alpha \cdot 10^6$(/K)	K (W/(m·K))	ν
Zirconia (ZrO_2)	151	10	2.09	0.3
Aluminum (Al)	70	23	204	0.3

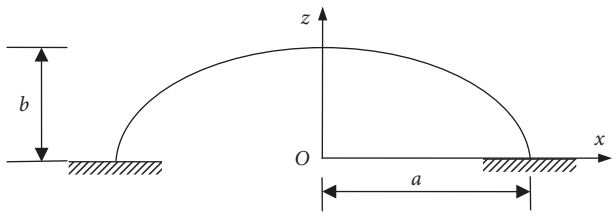

Figure 2: Configuration of the semielliptic curved beam with two ends clamped.

$$dS_0 = \frac{ds_0}{a} = J(\zeta)d\zeta, \tag{36}$$

where $J(\zeta) = \sqrt{\sin^2\zeta + \delta^2\cos^2\zeta}$ is the Jacobian of the transformation from the curvilinear domain to the parametric domain, $\delta = b/a$. Herein, the characteristic length is defined by $L = a$.

For the elliptic curved beam, we have

$$\cos\theta_0 = \frac{dx}{ds_0} = -\frac{\sin\zeta}{J}, \qquad \sin\theta_0 = \frac{dz}{ds_0} = \frac{\delta\cos\zeta}{J}. \tag{37}$$

Substituting equations (36) and (37) into equations (31)–(33), we can obtain differential equations defined in the parametric domain. In the view of symmetry of the structure, we select the half of the semielliptic curved beam ($0 \le \zeta \le \pi/2$) in the analysis. The boundary conditions can be written by

$$S(0) = 0, \quad U(0) = 0, \quad W(0) = 0, \quad \psi(0) = 0, \tag{38a}$$

$$U\left(\frac{\pi}{2}\right) = 0, \quad P_V\left(\frac{\pi}{2}\right) = 0, \quad \psi\left(\frac{\pi}{2}\right) = 0. \tag{38b}$$

It is difficult to find any analytical solutions of complicated ordinary differential equations (31)–(33) under boundary conditions (38a) and (38b) due to the inclusion of strong nonlinearity. So, the shooting method is used to search for the numerical solutions of the abovementioned two-point boundary value problem of the ordinary differential equations. First, the boundary value problem is transformed into an initial-value problem containing some unknown initial parameters. Then, the Runge–Kutta method is applied to search the solution of the initial problem, and the Newton–Raphson method is used to modify these unknown initial parameters until the boundary conditions at $\zeta = \pi/2$ are satisfied. Thus, the solution of the boundary value problem is obtained. The details about this numerical approach can be found in Reference [26]. For the FGM semielliptical curved beam only subjected to nonuniform thermal loading, we set $Q_x = Q_z = 0$ in equation (32).

First, we consider a semicircular beam ($\delta = 1$) made of full metal ($n \longrightarrow \infty$) and subjected uniform heating ($f_T = 1$). In Table 2 we list the values of nondimensional displacement $W(\pi/2)$ changing with the temperature rise parameter τ_i for some specified values of the slenderness parameter λ and make a comparison with those given by Li et al. [27], which shows a good agreement between the present results with those in the literature.

By specifying $\delta = 0.5$, characteristic curves of dimensionless displacement $W(\pi/2)$ and bending moment $m(\pi/2)$ of semielliptic FGM curved beam versus the power law index n are plotted in Figures 3 and 4, respectively, for different values of λ, where the results in solid lines and dotted lines are based on the Timoshenko and Euler curved beam theories, respectively. The difference between two types of lines reveals the influence of the shear deformation on the deformation and internal forces of the curved beam. Obviously, the shear deformation leads to the flexibility of the curved beam to be increased. But from the figures, we can find that the solid lines and dotted lines are almost coincident when the value of λ is less than 1/15, which means that the effect of the shear deformation weakens gradually and along with that the beam becomes thinner. For a given value of parameter of λ, displacement $W(\pi/2)$ increases with the increment of the power law index n, which accounts for the fact that a great value of n implies the curved beam has a large amount of the metal components which leads to a larger thermal expansion coefficient and lower stiffness.

Figures 5 and 6 illustrate the characteristic curves of the displacement $W(\pi/2)$ and bending moment $m(\pi/2)$ versus thermal load parameter τ_i, respectively, for $n = 0, 5, 10$ and $f_T = 5$. It can be seen that the increase in the value of the power law index leads to the increase in the deformation of the curved beam, which is due to the fact that the increase in the value of n results in the increase in the volume of the metal, in other words, the decrease in the equivalent elastic modulus of the curved beam.

As the second example, let us consider a closed FGM elliptic structure subjected to two pinching concentrated loads as shown in Figure 7(a). The nondimensional concentrated force can be expressed as $P = pa^2/(E_iI)$. Using the symmetry of the structure and loadings, only a quarter of the closed elliptic structure is analyzed, as shown in Figure 7(b). By selecting point A as the initial point of the parameter coordinate ζ, the whole domain of the problem is determined by $\zeta \in [0, \pi/2]$. The dimensionless boundary conditions are written as [28]

Table 2: Dimensionless displacement $W(\pi/2)$ of Al semicircular curved beam with two ends clamped under uniform temperature rise ($f_T = 1$).

λ		τ_i							
		50	100	150	200	250	300	350	400
1/30	Present	0.009	0.018	0.027	0.035	0.044	0.053	0.062	0.070
	Reference [27]	0.009	0.018	0.026	0.035	0.044	0.053	0.061	0.070
1/20	Present	0.020	0.040	0.059	0.079	0.098	0.117	0.136	0.154
	Reference [27]	0.020	0.040	0.059	0.078	0.098	0.117	0.135	0.154
1/10	Present	0.078	0.154	0.227	0.299	0.369	0.439	0.506	0.573
	Reference [27]	0.078	0.154	0.227	0.299	0.369	0.438	0.506	0.573

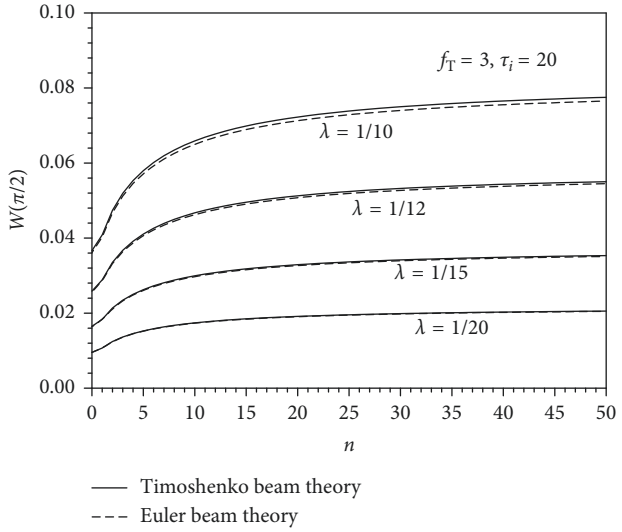

Figure 3: Dimensionless displacement $W(\pi/2)$ versus the power index, n, of the semielliptic FGM curved beam for different values of λ ($\delta = 0.5$).

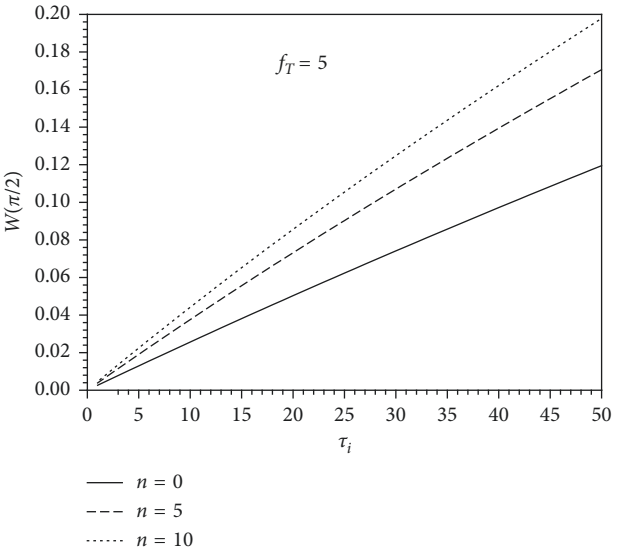

Figure 5: Variation of $W(\pi/2)$ versus τ_i with different values of n ($\lambda = 1/10$).

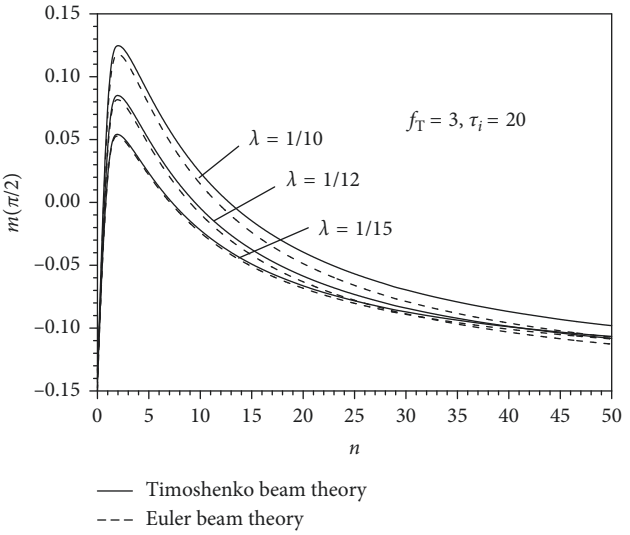

Figure 4: Dimensionless bending moment $m(\pi/2)$ of the semielliptic FGM curved beam versus the power index n for different values of λ ($\delta = 0.5$).

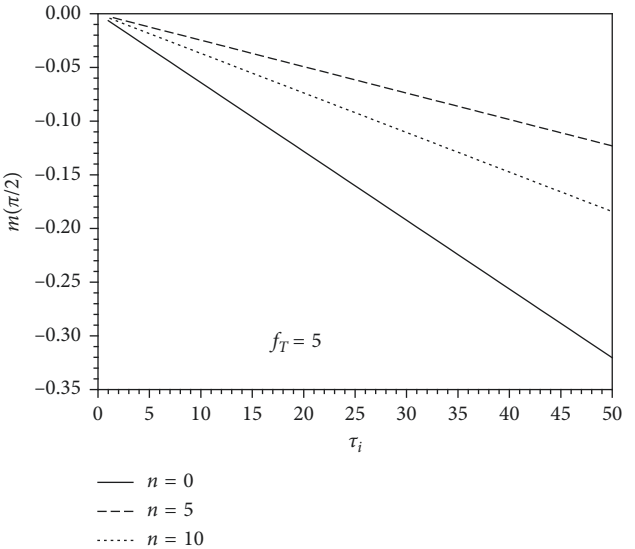

Figure 6: Variation of $m(\pi/2)$ versus τ_i with different values of n ($\lambda = 1/10$).

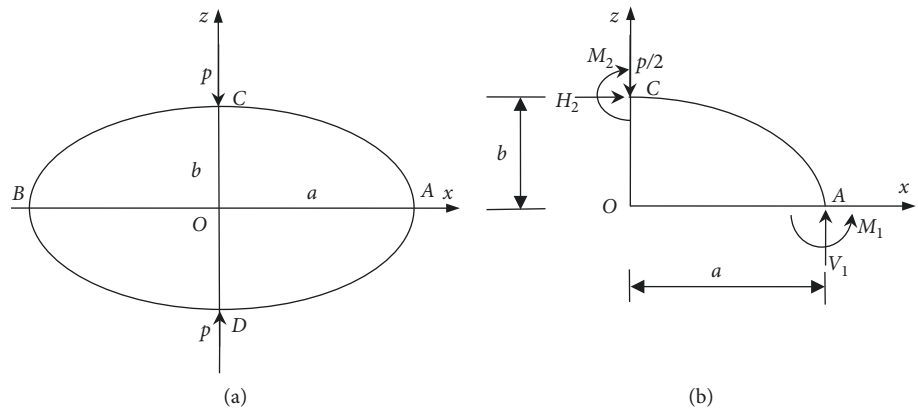

Figure 7: A pinched FGM elliptic structure model.

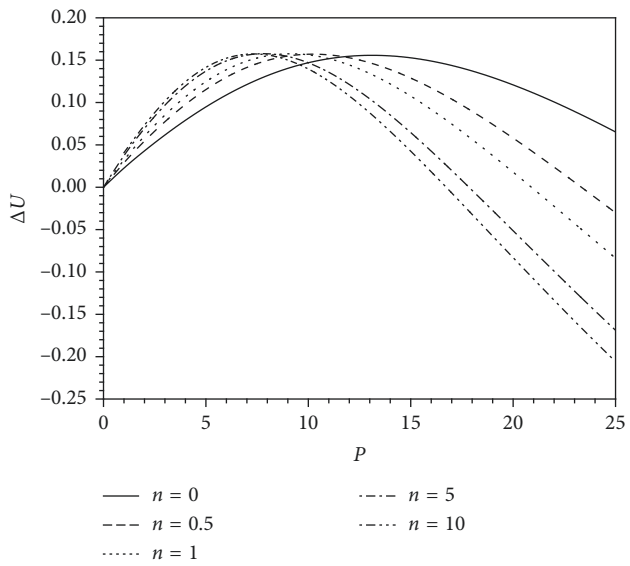

Figure 8: Variations of ΔU versus P with different values of n.

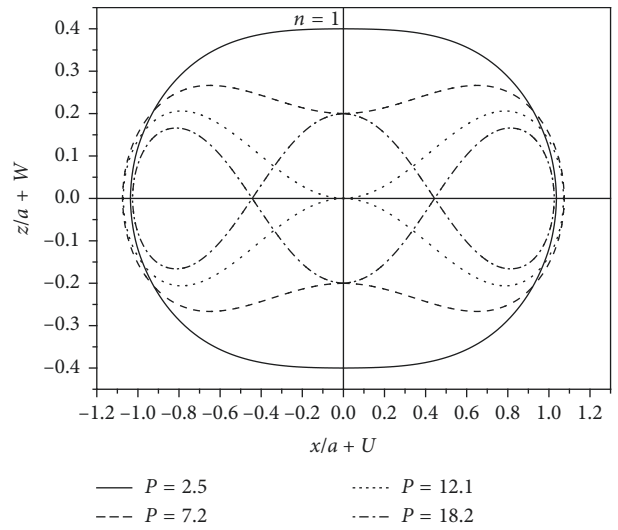

Figure 9: Equilibrium configurations of the elliptic curved beam for different values of P.

$$\begin{aligned} S(0) &= 0, \\ W(0) &= 0, \\ P_{\mathrm{H}}(0) &= 0, \\ \psi(0) &= 0, \end{aligned} \tag{39a}$$

$$\begin{aligned} U\left(\frac{\pi}{2}\right) &= 0, \\ P_{\mathrm{V}}\left(\frac{\pi}{2}\right) &= -\frac{P}{2}, \\ \psi\left(\frac{\pi}{2}\right) &= 0. \end{aligned} \tag{39b}$$

The relative horizontal displacements ΔU of point A and point B of the FGM elliptic curved beam versus the load P for different values of the power law index n are depicted in Figure 8. It can be seen that when the load increases, the relative horizontal displacements increase first and then decrease. This is because under the action of the vertical loads, the left and right sides of the elliptic ring will protrude. With the value of the load becoming larger and larger, point C and point D meet, and then the elliptic ring will contract in the horizontal direction.

In Figure 9, we have exhibited the equilibrium configurations of the curved beam for corresponding to different values of the pinching concentrated loads and for the power law index $n = 1$. As the load increases, the elliptic ring becomes more and more flat in the direction of the load. During the inception phase, the main deformations are compression and bending. When the value of load exceeds 12.1, point C gets to the negative y-axis, and point D gets to the positive y-axis. The main deformations become tensile and bending.

5. Conclusions

Based on the Timoshenko beam theory, geometrically nonlinear behaviors of the FGM curved beam with variable

curvatures have been researched by solving a system of seven coupled and strongly nonlinear ordinary differential equations. The material properties of the FGM curved beam are assumed to be varied continuously from the outer surface to the inner surface in the thickness direction. As a numerical example, geometrically nonlinear responses of a FGM semielliptic curved beam with two ends clamped under transversely temperature rise were obtained by using the numerical shooting technique. Characteristic curves of the displacement and bending moment versus the power law index for different slenderness and those versus thermal loading for different power law index were illustrated. From the numerical results, we find that the effects of shear deformation become significant along with the increase of the slenderness ratio, and the midspan deflection and bending moment of the curved beam are proportional to the thermal loading. In addition, some equilibrium paths and configurations of a FGM elliptic structure under two pinching concentrated loads were plotted. Numerical solutions in this paper may be the references to study geometric nonlinearity of FGM curved beams.

Appendix

Expressions of nondimensional coefficients in equations (19) and (20):

$$\begin{aligned}
\phi_1 &= \int_{-1/2}^{1/2} \frac{\psi_E}{1+\overline{\kappa}\eta} d\eta, \\
\phi_2 &= \int_{-1/2}^{1/2} \frac{\psi_E \eta}{1+\overline{\kappa}\eta} d\eta, \\
\phi_3 &= 12 \int_{-1/2}^{1/2} \frac{\psi_E \eta^2}{1+\overline{\kappa}\eta} d\eta, \\
\phi_4 &= \int_{-1/2}^{1/2} \psi_E d\eta,
\end{aligned} \tag{A.1}$$

$$\begin{aligned}
\beta_1 &= \int_{-1/2}^{1/2} \psi_E \psi_\alpha \psi_T d\eta, \\
\beta_2 &= \int_{-1/2}^{1/2} \psi_E \psi_\alpha \psi_T \eta \, d\eta,
\end{aligned} \tag{A.2}$$

where $\overline{\kappa} = \kappa_0 h$, $\eta = \rho/h$.

For elliptic curved beam,

$$\begin{aligned}
\kappa_0 &= \frac{b}{a^2 J^3}, \\
\overline{\kappa} &= \kappa_0 h = \frac{\delta\lambda}{J^3}.
\end{aligned} \tag{A.3}$$

Data Availability

The data used to support the findings of this study are available from the corresponding author upon request.

Conflicts of Interest

The authors declare that they have no conflicts of interest.

Acknowledgments

This work was supported by the National Natural Science Foundation of China (grant no. 11672260).

References

[1] H. Kurtaran, "Geometrically nonlinear transient analysis of thick deep composite curved beams with generalized differential quadrature method," *Composite Structures*, vol. 128, pp. 241–250, 2015.

[2] T. Q. Bui, A. Khosravifard, C. Zhang, M. R. Hematiyan, and M. V. Golub, "Dynamic analysis of sandwich beams with functionally graded core using a truly meshfree radial point interpolation method," *Engineering Structures*, vol. 47, pp. 90–104, 2013.

[3] T. V. Do, T. Q. Bui, T. T. Yu, D. T. Pham, and C. T. Nguyen, "Role of material combination and new results of mechanical behavior for FG sandwich plates in thermal environment," *Journal of Computational Science*, vol. 21, pp. 164–181, 2017.

[4] Y.-L. Pi and M. A. Bradford, "Non-linear in-plane analysis and buckling of pinned-fixed shallow arches subjected to a central concentrated load," *International Journal of Non-Linear Mechanics*, vol. 47, no. 4, pp. 118–131, 2012.

[5] Y.-L. Pi and M. A. Bradford, "Nonlinear elastic analysis and buckling of pinned-fixed arches," *International Journal of Mechanical Sciences*, vol. 68, pp. 212–223, 2013.

[6] L. Liu and N. Lu, "Variational formulations, instabilities and critical loadings of space curved beams," *International Journal of Solids and Structures*, vol. 87, pp. 48–60, 2016.

[7] M. Cannarozzi and L. Molari, "Stress-based formulation for non-linear analysis of planar elastic curved beams," *International Journal of Non-Linear Mechanics*, vol. 55, pp. 35–47, 2013.

[8] T. Pulngern, T. Sudsanguan, C. Athisakul, and S. Chucheepsakul, "Elastica of a variable-arc-length circular curved beam subjected to an end follower force," *International Journal of Non-Linear Mechanics*, vol. 49, pp. 129–136, 2013.

[9] L. S. Ma and D. W. Lee, "Exact solutions for non-linear static responses of a shear deformable FGM Beam under an in-plane thermal loading," *European Journal of Mechanics—A/Solids*, vol. 31, pp. 13–20, 2013.

[10] D.-G. Zhang, "Nonlinear bending analysis of FGM beams based on physical neutral surface and high order shear deformation theory," *Composite Structures*, vol. 100, pp. 121–126, 2013.

[11] H.-S. Shen and Z.-X. Wang, "Nonlinear analysis of shear deformable FGM beams resting on elastic foundations in thermal environments," *International Journal of Mechanical Sciences*, vol. 81, pp. 195–206, 2014.

[12] H. Asgari, M. Bateni, Y. Kiani, and M. R. Eslami, "Non-linear thermo-elastic and buckling analysis of FGM shallow arches," *Composite Structures*, vol. 109, pp. 75–85, 2014.

[13] M. Bateni and M. R. Eslami, "Non-linear in-plane stability analysis of FGM circular shallow arches under central concentrated force," *International Journal of Non-Linear Mechanics*, vol. 60, pp. 58–69, 2014.

[14] M. Bateni and M. R. Eslami, "Non-linear in-plane stability analysis of FG circular shallow arches under uniform radial pressure," *Thin-Walled Structures*, vol. 94, pp. 302–313, 2015.
[15] M. Kerdegarbakhsh, Y. Kiani, S. E. Esfahani, and M. R. Eslami, "Postbuckling of FGM rings," *International Journal of Mechanical Sciences*, vol. 85, pp. 187–195, 2014.
[16] H. Kurtaran, "Large displacement static and transient analysis of functionally graded deep curved beams with generalized differential quadrature method," *Composite Structures*, vol. 131, pp. 821–831, 2015.
[17] U. Eroglu, "Large deflection analysis of planar curved beams made of Functionally Graded Materials using variational iterational method," *Composite Structures*, vol. 136, pp. 204–216, 2016.
[18] B. Moghaddasie and I. Stanciulescu, "Equilibria and stability boundaries of shallow arches under static loading in a thermal environment," *International Journal of Non-Linear Mechanics*, vol. 51, pp. 132–144, 2013.
[19] N.-I. Kim, K.-J. Seo, and M.-Y. Kim, "Free vibration and spatial stability of non-symmetric thin-walled curved beams with variable curvatures," *International Journal of Solids and Structures*, vol. 40, no. 12, pp. 3107–3128, 2003.
[20] K. C. Lin and C. W. Lin, "Finite deformation of 2-D laminated curved beams with variable curvatures," *International Journal of Non-Linear Mechanics*, vol. 46, no. 10, pp. 1293–1304, 2011.
[21] A.-T. Luu and J. Lee, "Non-linear buckling of elliptical curved beams," *International Journal of Non-Linear Mechanics*, vol. 82, pp. 132–143, 2016.
[22] T.-A. Huynh, A.-T. Luu, and J. Lee, "Bending, buckling and free vibration analyses of functionally graded curved beams with variable curvatures using isogeometric approach," *Meccanica*, vol. 52, no. 11-12, pp. 2527–2546, 2017.
[23] T. Yu, H. Hu, J. Zhang, and T. Q. Bui, "Isogeometric analysis of size-dependent effects for functionally graded microbeams by a non-classical quasi-3D theory," *Thin-Walled Structures*, vol. 138, pp. 1–14, 2019.
[24] T. Yu, J. Zhang, H. Hu, and T. Q. Bui, "A novel size-dependent quasi-3D isogeometric beam model for two-directional FG microbeams analysis," *Composite Structures*, vol. 211, pp. 76–88, 2019.
[25] S. R. Li, X. Song, and Y. H. Zhou, "Exact geometrically nonlinear mathematical formulation and numerical simulation of curved elastic beams," *Engineering Mechanics*, vol. 21, pp. 129–133, 2004.
[26] S. Li, Y.-H. Zhou, and X. Zheng, "Thermal post-buckling of a heated elastic rod with pinned-fixed ends," *Journal of Thermal Stresses*, vol. 25, no. 1, pp. 45–56, 2002.
[27] S. R. Li and F. X. Zhou, "Geometrically nonlinear model and numerical simulation of elastic curved beams subjected to mechanical and thermal loads," *Chinese Journal of Mechanical Engineering*, vol. 25, pp. 25–28, 2008.
[28] N. Tayşi, M. T. Göğüş, and M. Özakça, "Structural analysis of arches in plane with a family of simple and accurate curved beam elements based on Mindlin-Reissner model," *Journal of Mechanics*, vol. 27, no. 1, pp. 129–138, 2011.